

**Original scientific paper**

*Received: 03.08.2023*

*Accepted: 11.10.2023*

**UDK:674.02:004.932.4**

**ASSESSING SHEAR STRAIN DISTRIBUTION IN WOOD UNDER IMPACT USING  
THE DIGITAL IMAGE CORRELATION METHOD**

**Mojtaba Hassan Vand<sup>1</sup>, Jan Tippner<sup>1</sup>**

<sup>1</sup>*Mendel University in Brno, Czech Republic  
Faculty of Forestry and Wood  
e-mail: xhassanv@mendelu.cz*

**ABSTRACT**

The demand for bio-based materials across various industries is growing fast, and it necessitates a comprehensive study of the high-rate loading effects on wood. While the 3-point impact bending test is commonly employed for evaluating material behavior, determining the strain distribution of the specimen remains challenging due to the fact that the impact takes place over a short period of time and that it requires specialized equipment and methods. Additionally, wood's heterogeneous nature and orthotropic structure make it difficult to identify the location of the highest shear strain. This research explores the potential of digital image correlation methods to determine the shear strain distribution in a wooden beam subjected to impact. The study determined the maximum shear strain in beech wood (*Fagus sylvatica* L.) and investigated the progressive pattern of shear strain during impact. The results demonstrate that, with appropriate equipment, the digital image correlation method can effectively determine the shear strain distribution during impact loading.

**Key words:** impact loading, shear strain, digital image correlation method

**1. INTRODUCTION**

Wood's mechanical properties can be considered an orthotropic material, which depends on the three anatomical directions and also on the other natural individual characteristics of it (Glass et al., 2013). There are comprehensive studies about the mechanical properties of wood in the static state, which commonly study the behavior of the wood by tension, compression, and shear tests in the three anatomical directions, and the results are mainly based on the determination of the mechanical properties such as Young's moduli, shear moduli, and Poisson's ratios (Clauß, Pescatore, Niemz, 2014), however, the number of studies for high-rate loading is significantly less than experimental studies for static loading (Poloco er et al., 2018). The three-point bending test is a common testing method for studying the mechanical behavior of materials under impact and high-rate loading (Marur, Simha, and Nair, 1994). It should be stated that different parameters, such as type of species (Jacques et al., 2014) and moisture content (Skaar, 2012), can affect the behavior of the wood under loadings, and the severity of the effect can be significant. The loading rate effect on the behavior of wood has been investigated in laboratories for many years (Johnson, 1986), but this task has many obstacles to overcome since the deformation of a sample is a global response, but the failure of the specimen is a local phenomenon, and an increase in the loading rate makes the failure more local (Yu and Jones, 1997). Due to the relative complexity of the impact loading and the lack of possibility for using connected sensors, non-contact methods are better and more advantageous. The digital image correlation method (DIC) is one of these non-contact methods. DIC is a robust optical method for displacement measurement and strain calculation based on image processing (Zhang and Arola, 2004). Due to its unique advantages, it has been used for various biomaterials; especially wood (Haldar et al., 2011). Although DIC has been used to evaluate strain distribution static (low-rate) loading tests,

analyzing wood samples under impact loading was not studied adequately as static tests (Dave et al., 2018).

During the bending of a beam, a region parallel to the beam's longitudinal axis would be created in which all of its points have no longitudinal strains (Beer, Johnston, and DeWolf, 2002). This hypothetical line is called the neutral axis, located at the centroid of the beam cross-section for homogeneous isotropic materials (Gere and Timoshenko, 1997). For wood, a heterogeneous, orthotropic material, the neutral axis would be near the centroid of the beam but not on it (Betts, Miller, Gupta, 2010). The location of the neutral axis for wood is not a clear straight line but a jagged line with curves, and the location of this axis varies along the beam (Davis, Gupta, Sinha, 2012). However, these studies were for static bending tests, and there are necessities for measuring the shear strain of beams under impact loading. The effectivity and potential of the DIC for measuring the shear strain of wood under high-rate loading were measured in this research, and the effect of the moisture content on the maximum shear strain was shown.

## 2. TESTS AND MEASUREMENTS

### 2.1 Experiments

Beech lumber (*Fagus sylvatica* L.) was provided by a local sawmill wood supplier in Brno, Czech Republic. A deliberate selection process was employed to use lumber from various trees due to the fact that the wood of different trees of the same species differs from each other. From the purchased raw material, the test samples were prepared for impact testing. These specimens were 20\*20\*300 mm (longitudinal × radial × tangential direction). A thorough visual inspection was conducted to discard samples with knots and defects. The prepared defect-free specimens were categorized into two distinct groups: the first group as the higher moisture content group (H-Group), and the second as the lower moisture content group (L-Group). The L-group specimens were stored in an environment maintained at 20°C and 65% relative humidity in order to reach a balanced moisture content of 12% of equilibrium moisture content (EMC). Conversely, the H-Group specimens underwent a process involving submerging in water for several days, followed by storage in a sealed chamber with elevated humidity levels, resulting in 56% of the EMC. Figure 1 shows a schematic of the dimensions of the specimens and the impact test boundary conditions.

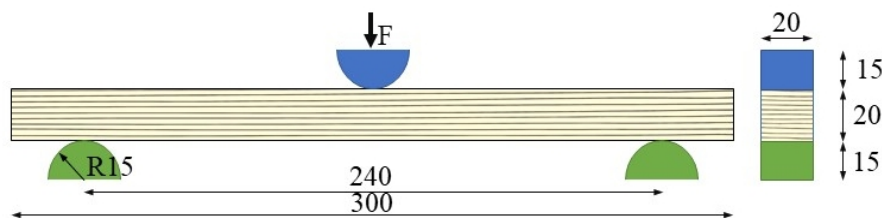


*Figure 1: A schematic of the test samples*

After preparation of the test samples, the specimens were tested in the Josef Ressel Research Center (Mendel University in Brno, Út chov, Czech Republic). The test was carried out on the drop-weight impact testing machine DPFest 400 (Labortech s.r.o., Czech Republic). The impact test was in strict adherence to established Czech standards ( SN 490115, 1979) and ( SN 490117, 1980). The tests were done in a common temperature room ( $\approx 20$  °C). The test is a high-rated 3-point bending test with the same conditions. The weight and the initial height of the hammer were 9.5 kg and 815.7 mm, respectively, making it able to provide 72.4 J of potential energy for the impact. The accuracy of the location of the hammer was 10–5 m. Both ends of the samples were on the fixed supports, and the hammer enforced the loading on the center of the samples. Half of the specimens from each group were tested in the radial direction and the other half in the tangential direction to consider the effect of the growth rings.

## 2.2 Recording equipment and considerations

Recognizing the clear influence of the random speckled pattern on the accuracy of the result of DIC (Pan, 2011), a speckled pattern was created on the surface of the samples. Due to the extreme high speed of the process of the impact, a set of high-speed (HS) equipment is used. The HS equipment was made up of two cameras. For lower resolution (1024×672 Px), a Photron Fastcam SA-X2 1000K-M2 with a cell size of 20 μm equipped with a lens Nikon Micro-Nikkor G and two teleconverters was used. For higher resolution (2048×600 Px), an Olympus i-SPEED 726R camera with a cell size of 13.5 μm equipped with a Nikon Macro-Nikkor lens was used. The frame rate of both cameras was 50000 fps. Since the light setting has a clear effect on the quality of the ultimate result, the texture contrast on the captured surface was enhanced by two high-speed MultiLED QT light sources. Acknowledging the critical significance of precise alignment of the camera and the specimens, both cameras were positioned horizontally to ensure alignment with the specimens' longitudinal axis; consequently, their captured images were parallel to the surface of the specimens, thereby securing the integrity of the output.

## 3. DIC EVALUATION

The next step, after recording the impact, was the processing of the images. For this task, highly effective software called Vic-2D v. 2010 (Correlated Solutions Inc., USA) was used. Although the Vic-2D software can determine the conversion factor by using simple scale calibration, there is no need for conversion factors since the strain has no unit. Lagrange notation was used for the computation of the strain tensors. The lowest possible displacement field of 3×3 points and the strain filter size of 5×5 points were applied. The standard correlation with the same image was used. Figure 2 illustrates an output image of the camera being used as the input for the Vic-2D software.

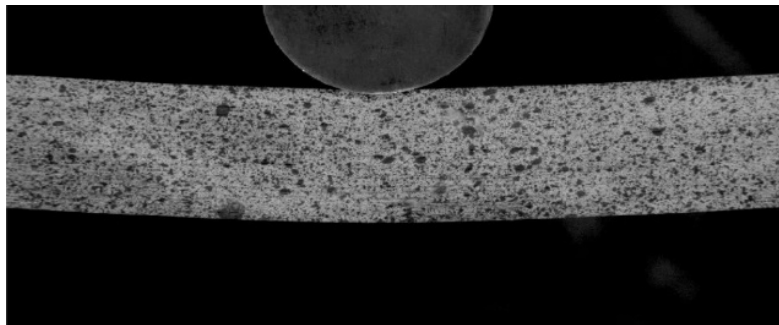


*Figure 2: An illustration of an output image*

Despite the many distinctive advantages of the DIC, it has certain challenges and limitations for the evaluation of the impact bending test. The first limitation is a lack of ability to evaluate the region near the hammer since the movement of the hammer from outside the region of the sample causes considerable local compression, causing the loss of data points adjacent to the hammer impact point. The second limitation emerges for the processing of images after crack initiation. The relative location of the pixels drastically changes after a crack, consequently causing errors and losing the output's accuracy. However, our main interest is the period leading up to crack initiation, where DIC provides valuable information.

The bending of the beams at any loading rate always creates a neutral axis on the beam. This axis represents a surface wherein all of the points are not under tension or compression, and the normal strain is zero. On the other hand, not only is the shear strain present on the neutral axis, but its optimum values are also on this axis at two points near the longitudinal center of the beam (Hibbeler, 2013). For isotropic homogenous material, the neutral axis can be determined easily since it is on the centroid; however, for heterogeneous anisotropic material, determination of the neutral axis is not straightforward. The varying grain patterns and knots located throughout wood due to the natural origin of wood make wood anisotropic and non-homogeneous, making the pinpointing of the neutral axis a challenging task (Jeong, Zink-Sharp, Hindman, 2010). Knowledge of the true location of the

neutral axis would facilitate a better understanding of the mechanical behavior of beams, and it is vital for the calculation of the maximum shear strains (Beer, Johnston, DeWolf, 2002). In essence, to find the neutral axis, the results of the longitudinal strains should be evaluated, and the area with zero strain defines the neutral axis. Figure 3 depicts the longitudinal strain results of the bending wood, and the approximate neutral axis can be seen as the zero strain area. By setting the inspecting polyline option in this area, the shear strain on the neutral axis can be derived. Figure 4 shows the shear strain pattern of the wooden beam.

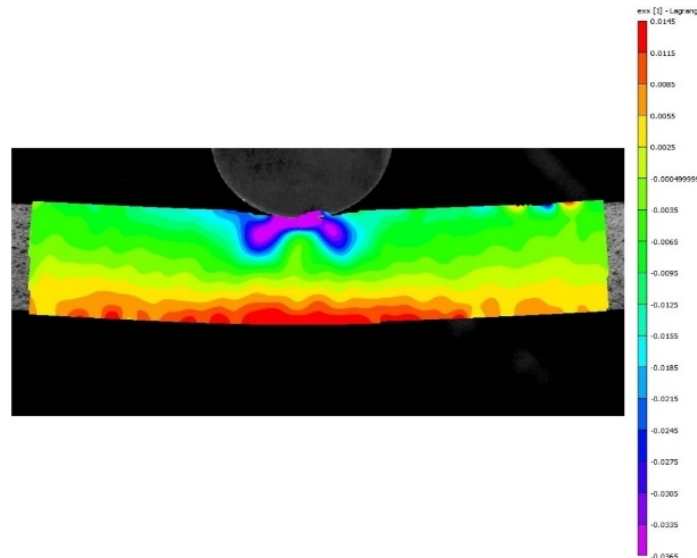


**Figure 3:** The longitudinal strain pattern of one specimen before crack initiation

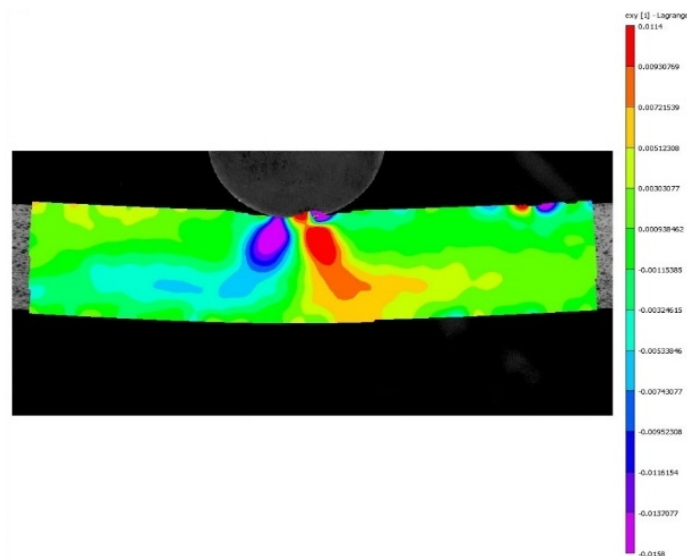


**Figure 4:** The shear strain pattern of one specimen before crack initiation

#### 4. RESULTS AND CONCLUSION

By processing the test records, the shear strain values on the neutral axis were determined. Figures 5 and 6 depict the shear strain curves for both the L-group and H-group, where the individual test results are the light shadow curves, while the red curve signifies the collective median value of all tests within the respective groups.

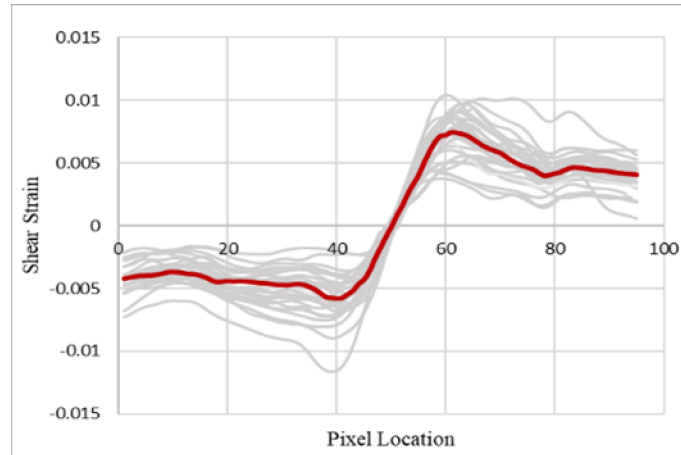


**Figure 5:** The shear stress patterns on the neutral axis of the central region of the L-Group samples

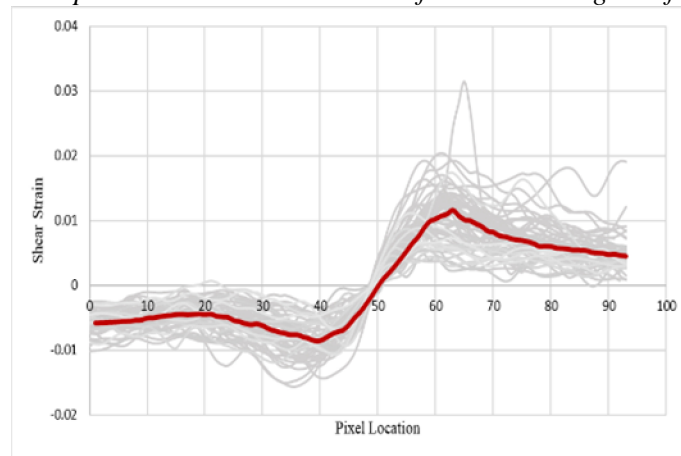


**Figure 6:** The shear stress patterns on the neutral axis of the central region of the H-Group samples

Another ability of the DIC for measuring the shear strain of the impact is its measurement at all of the moments of the impact. Figure 7 illustrates the value of the shear strain at the points located on the neutral axis of one specimen. The value of the maximum shear strain increases up to the crack initiation during this time. However, the increase in shear strain has no clear pattern except for the overall increase.

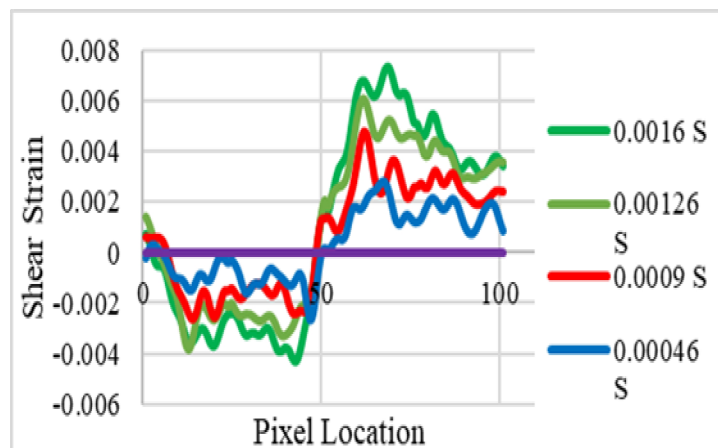


**Figure 7:** The shear stress patterns on the neutral axis of the central region of one of the tests during different moments of the impact

Another important aspect of the result is its distribution. Figure 8 shows the boxplot of the optimum points of the shear strain for both groups. It can be seen that the H-group clearly shows a higher level of shear strain before breaking.

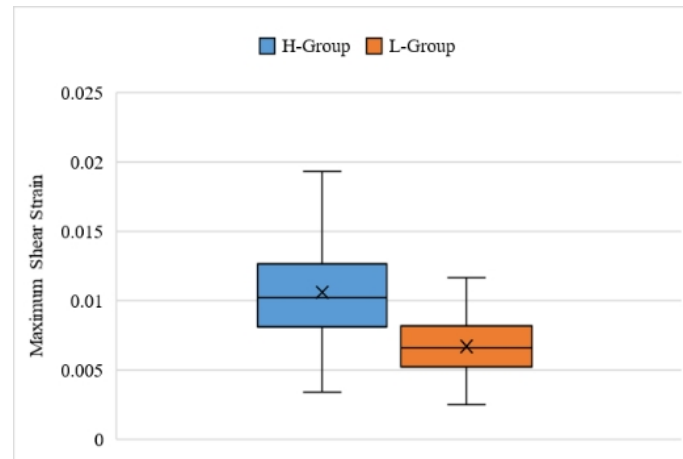


**Figure 8:** Boxplot of the shear strain optimum points

It should be mentioned that for measurement of the values in impact tests, the choices for tools and methods are limited, and this lack of variety of tools magnifies the importance of DIC in these types of tests. The DIC has great potential as a non-contact method for measuring strains for high-rate loading. However, due to the high variability of the values for each sample, it is recommended to have a large number of specimens.

### Acknowledgements

This work was supported by the Ministry of Education, Youth and Sports in the Czech Republic [Grant Number #LL1909, ERC CZ]

### REFERENCES

- [1] Beer, F. P., Johnston, E. R., DeWolf, J. T. (2002): "Mechanics of Materials." Singapore: McGraw-Hill.
- [2] Betts, S.C., Miller, T.H. and Gupta, R. (2010): "Location of the Neutral Axis in Wood Beams: A Preliminary Study." *Wood Material Science and Engineering*, 5(3-4), pp. 173-180.
- [3] Clauß, S., Pescatore, C., Niemz, P. (2014): "Anisotropic Elastic Properties of Common Ash (*Fraxinus excelsior* L.)." *Holzforschung*, 68(8), 941-949.
- [4] SN 490115 (1979): "Wood. Detection of Static Bending Strength." Czech Standards Institute, Prague, Czech Republic.
- [5] SN 490117 (1980): "Wood. Impact Strength in Bending." Czech Standards Institute, Prague, Czech Republic.
- [6] Dave, M. J., Pandya, T. S., Stoddard, D., Street, J. (2018): "Dynamic Characterization of Biocomposites Under High Strain Rate Compression Loading with Split Hopkinson Pressure Bar and Digital Image Correlation Technique." *International Wood Products Journal*, 9(3), 115-121.
- [7] Davis, P. M., Rakesh, G., Arijit, S. (2012): "Revisiting the Neutral Axis in Wood Beams." *Holzforschung*, Vol. 66, pp. 497–503.
- [8] Glass, S. V., Cai, Z., Wiedenhoft, A. C., Ross, R. J., Wang, X., Hunt, C. G., Rammer, D. R. (2013): "Wood Handbook-Wood as an Engineering Material." CreateSpace Independent Publishing Platform; Centennial edition.
- [9] Gere, J., Timoshenko, S. *Mechanics of Materials* (4th edition). PWS Publishing Co, 1997.
- [10] Haldar, S., Gheewala, N., Grande-Allen, K. J., Sutton, M. A., Bruck, H. A. (2011): "Multi-Scale Mechanical Characterization of Palmetto Wood Using Digital Image Correlation to Develop a Template for Biologically-Inspired Polymer Composites." *Experimental Mechanics*, 51(4), 575-589.
- [11] Hibbeler, Russell C. (2013): "Mechanics of Materials." United Kingdom: Pearson Education.

- [12] Jacques, E., Lloyd, A., Braimah, A., Saatcioglu, M., Doudak, G., Abdelalim, G. (2014): "Influence of High Strain-Rates on the Dynamic Flexural Material Properties of Spruce–Pine–Fir Wood Studs." *Canadian Journal of Civil Engineering*, 41(1), 56-64.
- [13] Jeong, G. Y., Zink-Sharp, A., & Hindman, D. P. (2010). Applying digital image correlation to wood strands: influence of loading rate and specimen thickness.
- [14] Johnson, W. (1986): "Historical and Present-Day References Concerning Impact on Wood." *International Journal of Impact Engineering*, 4(3), 161-174.
- [15] Marur, P. R., Simha, K. R. Y., Nair, P. S. (1994): "Dynamic Analysis of Three Point Bend Specimens Under Impact." *International Journal of Fracture*, 68(3), 261-273.
- [16] B. Pan, "Recent Progress in Digital Image Correlation. *Experimental Mechanics*, 51(7), 1223–1235, 2011.
- [17] Poloco er, T., Kasal, B., Stöckel, F., Li, X. (2018): "Dynamic Material Properties of Wood Subjected to Low-Velocity Impact." *Materials and Structures/Materiaux et Constructions*, 51(3). <https://doi.org/10.1617/s11527-018-1186-z>
- [18] Skaar, C. (2012): "Wood-Water Relations." Springer Science & Business Media.
- [19] Yu, J. L., Jones, N. (1997): "Numerical Simulation of Impact Loaded Steel Beams and the Failure Criteria." *International Journal of Solids and Structures*, 34(30), 3977-4004.
- [20] Zhang, D. M., Tan, Y. H., Gao, S. X. (2014): "Evaluation of the Maximum Shear Strain of Clamped Composite Plate Using Digital Image Correlation Method." *Advanced Materials Research*, 945, 427-431.
- [21] Zhang, D. S. & Arola, D. D. (2004): "Applications of Digital Image Correlation to Biological Tissues." *Journal of Biomedical Optics*, 9(4), 691-699.